Journal of Engineering Science and Technology Review 16 (2) (2023) 116 - 122

Research Article

JOURNAL OF
Engineering Science and Technology Review

www.jestr.org

Influence of Patching Length on the Flexural Behaviour of Patched Reinforced Concrete Beam

Halwan Alfisa Saifullah*, Agus Supriyadi, Annisa Rizki and Stefanus Adi Kristiawan

SMARTCrete Research Group, Civil Engineering Department, Universitas Sebelas Maret, Jl. Ir Sutami No. 36A Surakarta 57126, Indonesia

Received 11 August 2022; Accepted 7 April 2023

Abstract

Reinforced concrete (RC) structures can experience damage due to material degradation, overloading, and other circumstances. Damage can take the form of spalling and delamination. One of the straightforward techniques to repair those localized damages is patching. Several types of materials can be used as patching material, one of which is Unsaturated Polyester Mortar (UPR)-Mortar. The UPR-mortar possesses low elastic modulus, high early strength, and adequate bond strength. However, only a few studies investigate the efficacy of employing the UPR-mortar patching to rehabilitate reinforced concrete structures. The current study uses experimental and numerical methods to examine how patching with UPR-mortar affects the flexural performance of reinforced concrete beams. Loading tests on RC beams with and without patching repair were carried out in the laboratory. During the loading test, the load and midspan deflection, strain development of the flexural reinforcements, and flexure crack evolution were monitored. Numerical simulations were also performed to validate the experimental results and further investigate the beam behavior with varying patching lengths. The results indicate that the remediation of RC beam with UPR-mortar patching can restore and boost flexural strength. Furthermore, when the patching length exceeds the maximum beam moment zone's length, the beam's flexural capacity increase becomes more apparent.

Keywords: crack, flexure, patching, unsaturated polyester resin (UPR) mortar, reinforced concrete

1. Introduction

The performance of reinforced concrete structural components tends to deteriorate as the structure ages owing to internal and external factors. Scaling, disintegration, erosion, reinforcement corrosion, delamination, spalling, alkali-aggregate reactions, and concrete cracking are examples of concrete structural deterioration [1-6]. Creep and shrinkage effects may also increase deformation and cracks. Besides, unexpected occurrences such as earthquakes and fires may also cause damage to structures [7-9]. Furthermore, damage to structural components throughout the building's service life may be worsened by changes in the building's purpose, resulting in a substantial increase in load without adequate structural repairs and strengthening. Older reinforced concrete structures often suffer from corrosion of the reinforcing and concrete cover peeling. The passive layer of concrete that covers the reinforcement may deteriorate due to carbonation and chloride attack resulting in reinforcement corrosion. Corroded reinforcement expands in volume and exerts pressure in all directions, causing the surrounding concrete to experience tensile stress. This tensile stress results in cracking and concrete cover peeling away. The reduction in reinforcement area due to corrosion and loss of bond between the reinforcement and the surrounding concrete will undoubtedly affect the structural integrity and significantly reduce the stiffness and flexural strength of the beam. This will have impacts on the service life, safety, and reliability of concrete structures [10-15].

It is necessary to do repair and rehabilitation work to improve structural integrity, lengthen service life, enhance safety, and boost durability. In some cases, repairing the deteriorated concrete may be a more cost-effective choice than replacing the degraded concrete with a new structure. Efforts to repair structural damage are carried out to restore the structure's load-bearing capacity and improve resilience to physical or chemical attacks. Often the repair actions are also followed by increasing the structural capacity [9, 16-20]. Numerous factors must be considered while determining the repair technique, including its efficacy, cost, simplicity of use, and durability. The chosen damage repair must be able to withstand and prevent further degradation. Therefore, it is necessary to investigate the cause of the damage before selecting a repair method. Grout, mortar, concrete, sprayed concrete, resin-based material, externally bonded steel plate, and composite materials are some available repair materials. Currently, numerous waste materials (such as fly ash, ferrosilicon, and silica fume) are employed as a partial replacement for cement to reduce environmental issues and enhance the performance of concrete or mortar mixes [21, 22]. The success of a repair job is contingent upon the quality of the materials utilized, the implementation methods employed, and ultimately the work performed by skilled operators under the supervision of experienced supervisors who fully grasp the rationale behind the techniques used [23-25]. Several technical documents, such as ACI 546R-14 [26] and EN 1504-9 [27], provide basic guidance for selecting and using materials and methods for repairing concrete structures.

Patching is a well-established technique for repairing localized damage to reinforced concrete structures, such as spalling and delamination. This procedure involves the

*E-mail address: halwan@ft.uns.ac.id
ISSN: 1791-2377
doi:10.25103/jestr.162.15

removal of damaged concrete and reinforcement bars, installing new reinforcements (if necessary), and applying repair mortar to the repaired area. This approach offers lower cost, faster and more efficient execution, and simplicity in application. Numerous factors influence the performance of an RC structure repaired using the patching method, including surface preparation of base concrete, rebar cleanliness, mechanical properties of repair materials, and patching area. When selecting a patching material, it is critical to consider the compatibility of the repair material with the repaired material to limit the occurrence of cracks and the separation of the repair material from the parent material [28-37]. Repair materials can be classified into cement-based materials, polymer mortar-based materials, polymer concrete-based materials, organic polymer-based materials, and composite materials [2]. The authors have developed and formulated a composite material composed of unsaturated polyester resin (UPR), sand, cement, and fly ash. In the absence of water in the repair material mixture, cement and fly ash are utilized as fillers, while UPR is the binding agent. UPR-mortar can produce a patch repair with a low modulus of elasticity and a high initial strength. The UPR content affects the flexural properties of UPR-mortar, especially at an early age. Higher UPR content tends to produce mortar with faster flexural strength development, which may be attributed to the reaction heat generated by the resin and its initiator during the cross-linking process. However, UPR content does not affect the flexural properties of UPR-mortar at later ages [38]. The lower ratio of the UPR-mortar's elastic modulus to the parent concrete will generate lower stresses in the patched repair zone than the concrete. This will prevent the occurrence of initial cracks in the repaired area. The repair material also provides sufficient early strength, ensuring the structural performance can be recovered quickly to resist external loading. Furthermore, the developed UPR-mortar has an adequate bond strength to withstand the interface's tensile, peeling, or shear stresses, thereby avoiding delamination between the parent concrete and repaired material. Due to the low modular but high strength ratio of combined UPR-mortar and substrate concrete, the bond strength is determined by the strength of the substrate concrete [39].

Research on the flexural behavior of reinforced concrete beams is very important because most reinforced concrete structures are designed to achieve ductile failure [40]. The authors have also conducted some experimental studies examining the efficacy of utilizing the UPR-mortar to rehabilitate the flexural capacity of reinforced concrete beams. The investigations have been performed by employing UPR-mortar to patch a replicated damage in the maximum flexural tensile zone of the RC beam. The presence of UPR-mortar influenced the formation of flexural cracks, strength, and rigidity of the beam. Cracks began to develop outside the repaired area. This contrasted with the observation results on the unrepaired beam, which show the initiation of flexural cracks in the maximum moment zone. The crack intensity and deflection of the patched beam were less than those of the normal beam. Patching repair using UPR-Mortar could restore and even increase the flexural capacity of reinforced concrete beams [41]. Furthermore, the cracking moment and flexural capacity of patched reinforced concrete beams increased with patch thickness [42]. Loading tests were also performed at the structural level on one-way and two-way slabs patched with UPR-mortar. The experimental results showed that UPR-mortar could restore both strength and stiffness, as well as increase the ductility of the patched RC slabs [43-45]. Only a few more studies examined the performance of beams patched with UPR-mortar [46]. Therefore, further investigations are still needed to evaluate other parameters affecting the efficacy of UPR-mortar as a repair material of the structure.

The present research experimentally and numerically investigates the influence of patching with UPR-mortar on the flexural behavior of RC beams. Loading tests in the laboratory were carried out on RC beams with and without patching repair. During the loading test, the flexural cracking and ultimate strengths, deformation, and crack development of RC beams were monitored during the loading test. The observed and measured performance of beams was then replicated and examined in detail using non-linear finite element software. The patching effects are further explored in this study using numerical simulations of beams with varying patching lengths.

2. Experimental Investigation and Numerical Modelling

2.1. Materials and Properties

This study used ordinary concrete containing 388 kilograms of cement, 225 kilograms of water, 771 kilograms of sand, and 941 kilograms of coarse aggregate per cubic meter. Cylindrical specimens with a diameter of 150 mm and a height of 300 mm were prepared for the compressive strength and splitting tensile strength tests following ASTM (American Society for Testing and Materials) C-39 and C-496. The average concrete compressive and tensile strengths at the loading age were 30.82 Mpa and 2.59 Mpa, respectively. The steel material used for reinforcement bar of beam had a specified yield strength of 402 MPa. The UPR-mortar used as a repair material consists of 950 kilograms of sand, 808 kilograms of cement, 143 kilograms of fly ash, 475 kilograms of UPR, and 24 kilograms of hardener per meter cubic. YUKALAC®157 BQTN-EX, an unsaturated orthophtalic type resin produced by polymerizing di-carboxylic acids with glycols, was used as the UPR in this study. The strength of repair materials was tested on cube specimens of 50x50x50mm in accordance with ASTM C 579-01. At the age of loading test, the average compressive strength of the UPR mortar was 72.50 MPa obtained from a test following ASTM C 579-01. The UPR mortar also had relatively lower elastic modulus (13.41 GPa) and higher tensile strength (20 MPa) than the parent concrete.

2.2. RC Beam Specimens

Two types of reinforced concrete beams with a size of 150x250x2000 mm were cast and tested for investigation purposes, i.e., repair beam (RB) and normal beam (NB). All beams have the same length, cross-sectional area, and reinforcement configurations, as indicated in Figure 1. The shear capacity of the beam was designed to be greater than its flexural capacity to ensure the flexural failure mode. Therefore, some web reinforcements with a diameter of 6 mm and a spacing of 100 mm were installed in the shear span of the beam. Longitudinal tension reinforcement consisted of two deformed bars with a diameter of 13 mm. In addition, two plain bars with a diameter of 6 mm were placed in the flexural compression zone to stabilize the rebar cage. Furthermore, beams were also planned to fail with flexural reinforcement yielding before concrete crushing in the upper flexural compression zone. The presence of a repair area distinguishes RB beam from NB beam. The RB beam had a patching layer with a thickness of 70 mm and a length of 400 mm located in the maximum moment zone. Meanwhile, the NB beam, which serves as a control beam, was not designed with a repair area. One day before the loading test, UPR-mortar was applied to the repair zone of the RB beam.

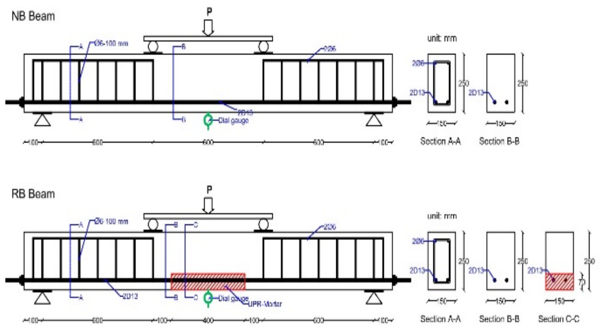

Fig. 1. Outline of the beam.

2.3. Testing of RC Beam

All RC beams were tested under monotonic four-point bending mode with a span of 1800 mm between the two supports and a constant moment region of 600 mm. In the constant moment zone, there is no shear force. As a result, this zone allows for observation of beam behavior under pure flexural loads. The beam specimens were tested at the age of 90 days. The loading test was performed with a load increment of 4 kN until the beam failed. The deflection of the beam, the development of longitudinal reinforcement strain, and the crack evolution were monitored during the loading test. A dial gauge was located at the beam midspan to measure the maximum deflection. The crack evolution was observed and checked manually for every load increment. The outline of the measurement system is illustrated in Figure 1.

2.4. Numerical Modelling

2.4.1. Constitutive Model of τhe Materials

Numerical modelling was carried out with the aid of the 3D ATENA Engineering software. The 3D nonlinear cementitious material 2 is employed to model concrete and UPR-mortar, where the complete equivalent stress-strain curve is shown in Figure 2. The curve comprises four distinct states. The first and second states indicate the behavior of concrete and UPR-mortar under tension. The ascending part up to the maximum stress demonstrates linear elastic behavior, whereas the descending portion shows the nonlinear softening model due to the capacity reduction. The two later states represent the uniaxial compression behavior of concrete and UPR-mortar. The initial portion of the ascending curve up to about 40% of the maximum stress exhibits a linear elastic behavior. After that, concrete undergoes significant damage at higher stresses until it reaches the ultimate value. Lastly, a nonlinear softening model after the peak is also used to characterize the decrease in capacity. On the other hand, longitudinal and web reinforcements were modelled using a reinforcement bilinear model, which exhibits elastic-perfectly plastic behaviour. Utilizing idealized curves for numerical analysis is much more stable. Steel plates were used to distribute the load at either the loading or support points to avoid the concentrated stresses that may affect the concrete fracture. For this purpose, a 3D elastic isotropic was used to model the steel plate, which is expected to behave elastically with unlimited strength during loading.

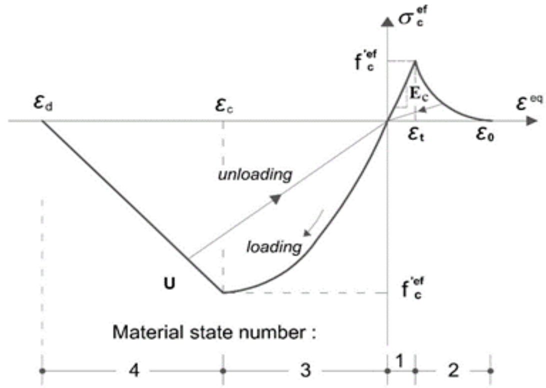

Fig. 2. Equivalent uniaxial stress-strain of concrete.

2.4.2. Modelling of RC Beams

Figure 3 illustrates solid 3D finite element meshes generated using a linear brick element type for normal and repair beams. For reasons of symmetry and numerical efficiency, the beams were modeled as half beams. The support was restrained against any horizontal movements. The same restraint was applied to the right cross section of the half beam model. The properties of the materials and their corresponding constitutive models used in this investigation are summarized in Table 1. Numerical simulations were conducted by applying a point load on top of the beam models at 1/3L from the support. The simulation was performed with a load increment step of 2 kN (about a half of the experimental loading) to capture more detail in the crack development process. The numerical simulation was extended to include identical beams with varying patching lengths.

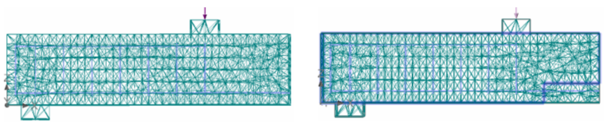

Fig. 3. Finite element model of normal beam (left) and repair beam (right).

Table 1. Properties of materials and their corresponding constitutive model.

Materials	f'c (MPa)	ft (MPa)	E (GPa)	Constitutive Model
Concrete	30.82	2.59	25.30	3D Non-Linear Cementitious2
UPR-mortar	72.5	20.00	13.41	3D Non-Linear Cementitious2
Steel plate	NA	NA	200.00	3D Elastic Isotropic

3. Results and Discussion

3.1. Cracks Pattern

Both normal and patched beams fail due to tension steel reinforcement yielding followed by concrete crushing. The crack development of the normal RC beam under flexural loading are shown in Figure 4. The normal RC beam exhibited the first flexural cracks at a load of 24 kN. The cracks developed in the constant moment zone of the beam, which was subjected to the highest flexural stresses. As the load increases, flexural cracks also occur in both shear spans of the beam and penetrate deeper into the flexural compression zone. After reaching the yielding load of 66 kN, the crack width increased rapidly. The flexural cracks are almost evenly distributed along the beam at this stage. The beam finally failed at a load of 83 kN.

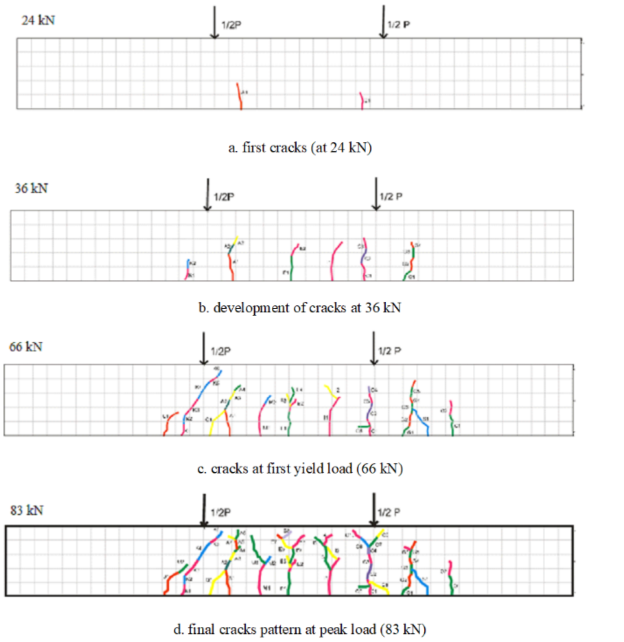

Fig. 4. Cracks development of normal beam.

Figure 5 depicts the crack development of the patched beam during the loading test. In contrast to the normal beam, the initial cracks of the patched beam appear outside the maximum moment zone at a load of 30 kN. The UPR mortars, with a higher modulus rupture than the concrete parent, can keep the patching area still uncracked until a certain load level. Several flexural cracks were observed in the repaired area at the yielding load of 71 kN. However, the cracks tended to terminate within the thickness of the UPR mortar and did not propagate vertically to the parent concrete. As also illustrated in Figure 5, only one advanced crack emerged above the repair zone, and it was not connected to any of the previous cracks within the repair area. The beam failed at a load of 85 kN. The crack intensity of the patched beam is less than that of the normal beam. The patched beam can better maintain the beam's rigidity in the post-cracking region. Furthermore, no delamination occurred between the repair material and the parent concrete. This demonstrates that the repair material provides sufficient bonding strength to preserve compatibility between the two materials under the applied load.

3.2. Load-Deflection Behaviour

The load-deflection curve can represent the correlation between deformation and crack formation. As more cracks form, the beam's stiffness decreases, leading to increased deformation for a given load. Figure 6 shows the relationship between the load and midspan deflection of RC beams. Generally, both the normal and patched RC beam shows a similar trend of the load-midspan displacement relationship. However, the patched beam shows a slightly lower stiffness than the normal beam due to the low modulus of elasticity of the UPR-mortar. During the early loading stage, RC beams undergo elastic deformation, and concrete cracks have yet to form. The occurrence of initial cracks at a load of 24 kN for the normal beam and 30 kN for the patched RC beam results in the stiffness reduction of the beams and decreasing slope of the load-deflection curves. The subsequent decrease in stiffness occurred when the longitudinal reinforcements experienced yielding at a load of 66 kN and 77 kN for the normal and patched beams, respectively. Following the passage of the yield load, tension reinforcement loses its function as a flexural crack width controller. A minor increase in load results in a considerable rise in deformation. The normal beam collapsed at an 83 kN load and a 25.1 mm deflection. On the other hand, the patched beam failed at a higher load of 85 kN and a more significant deflection of 29.5 mm. The reparation of RC beam using UPR-mortar not only restores but also increases the strength. The influence of UPR-Mortar repair on the performance of reinforced concrete beams will be discussed further in the next section using a parametric study with varied patching lengths.

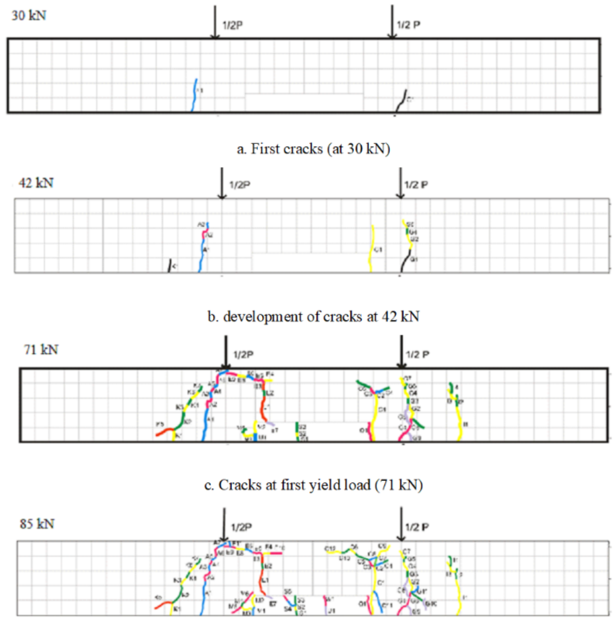

Fig. 5. Cracks development of repair beam.

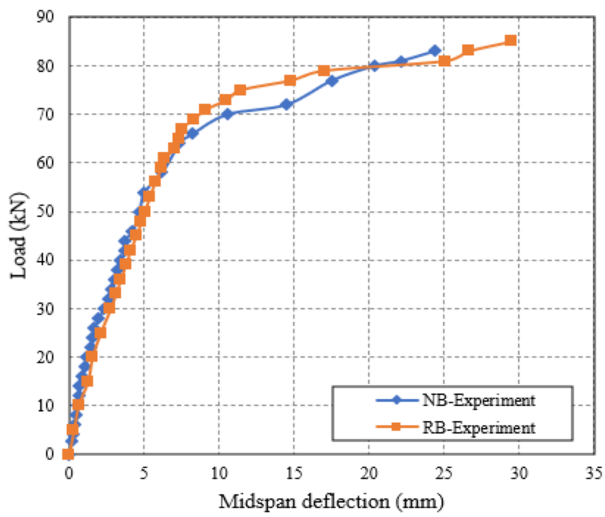

Fig. 6. Experimental results of load-midspan deflection.

3.3. Numerical Simulation

3.3.1. Validation of the Numerical Simulation and Experimental Result

The accuracy and reliability of the numerical model must be improved and validated by comparing the FEM results with the experimental test observations [47]. Figure 7 shows the comparison of the load-midspan deflection curve derived from experiments and numerical simulations. The numerical simulation can reproduce the yielding load, ultimate load, and associated deformations obtained in the experiment with differences of less than 10%. The more ductile behavior of the repair beam is also well simulated through numerical modeling. This indicates that numerical modeling using ATENA software has sufficient reliability in reproducing the flexural behavior of reinforced concrete beams both with and without UPR-Mortar patching repair. Numerical simulations were then utilized to further explore the beam's detailed behavior under bending load that experimental works cannot capture.

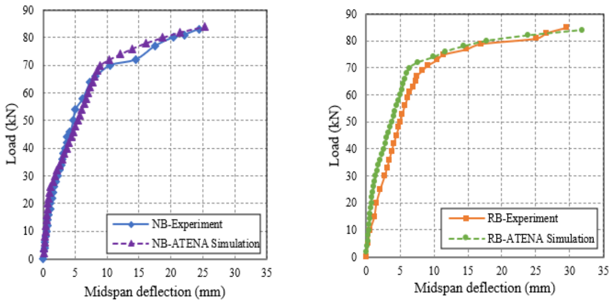

Fig. 7. Load-midspan deflection of normal beam model (left) and repair beam model (right).

The effects of patching on the beam behaviour can be explained using reinforcement stress and strain. The detailed stress and strain behaviour that occur in concrete and reinforcement can be determined through numerical analysis. Figure 8 illustrates the normal stress state of the beam reinforcement in the longitudinal direction at a given load level. The stress has a positive value when it is in tension and negative when it is in compression. The highest stress in the tension reinforcement occurs at the maximum moment zone in the normal beams. As the location gets closer to the supports, the flexure moment and tensile stress of reinforcement decreases. This is consistent with the visual observation results, showing that flexural cracks occurred first in the midspan, followed by cracks in other areas along the beam. On the other hand, the repair beam exhibits a distinct behavior. The maximum stresses do not occur in the maximum moment region but at the location close to the patching repair boundary in the shear span of beam. This is in accordance with the experimental findings, which indicate that the initial flexural crack occurs outside the region of maximum moment. The stresses in the maximum moment region are smaller than that of the normal beam, as also indicated in Figure 8. The presence of UPR-Mortar repair material causes this behavior. The lower elastic modulus and higher tensile strength of the UPR-mortar compared to the parent concrete results in less stress in the patched repair zone than the concrete. The repair area can maintain its rigidity up to a high load level, ensuring that the crack intensity in this area is not excessive.

As in the case of reinforcement stress, the details of reinforcement strain behavior can also be simulated numerically. Figure 9 shows the load-reinforcement strain relationship of the beam at the mid-span (1/2L) and the location just below the loading point (1/3L). The normal and repair beams have different load-reinforcement strain relationships at those two locations. At the midspan of the normal beam, the slope of the load-strain relationship curve changed multiple times as the load rose due to increased cracking and the yielding of steel reinforcement. On the other hand, the load-reinforcement strain relationship remains linear in the case of the repair beam, indicating that the reinforcement has not yielded until the beam failure. The identical strain behavior is observed in both normal and repair beams at locations below the loading point, starting from the initial loading until the reinforcement yielding. After the reinforcement yielding, both beams experienced a rapid increase in the flexural reinforcement strain. However, the patched beam exhibits more ductile behavior before failure.

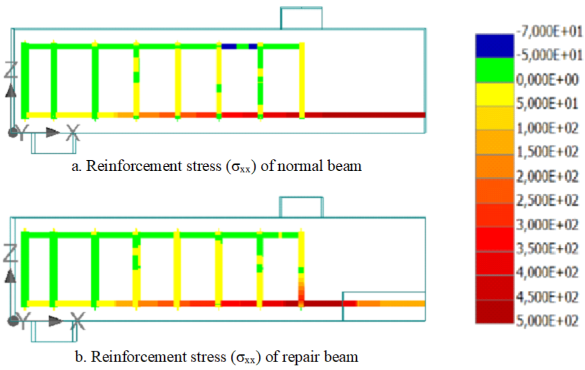

Fig. 8. Reinforcement stress.

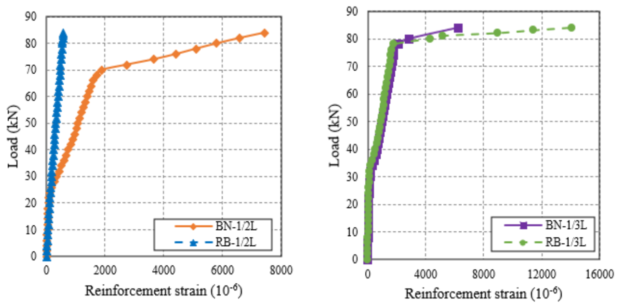

Fig. 9. Reinforcement strain at 1/2L and 1/3L.

3.3.2. Influence of Patching Length

It is expected that the behaviour of the patched beam will change as the geometry of the repair area changes. Previous study by the authors indicated that increasing patching thickness reduces cracking density and increases maximum load capacity. The current experimental results on an RC beam with a repaired length of 400 mm also demonstrated a rise in the flexural capacity. A parametric study was conducted to further investigate the effect of patching on the flexural behavior of reinforced concrete beams by varying the patching length. The patching lengths ranged from 0 to 700 mm, in which a beam with a patching length of 0 mm indicated the beam without repair or normal beam. The condition of normal stress at a given load level that occurs in longitudinal reinforcement of beams with varying patching lengths is depicted in Figure 10. In the case of normal beam, the maximum stress occurs in the region between the two loading points with the highest moment value. A different stress distribution appears in the patched beams. The utilization of patch repair can shift the location of maximum stress to the outer limit of the repair zone. As a result, the border region will first experience cracking and reinforcing yielding. The longer the patching length, the longer cracking and yielding of the beam reinforcement can be delayed. This certainly can improve the ductility and flexural capacity of the beam. Sahamitmongkol et al [46]. observed a similar trend in their investigation.

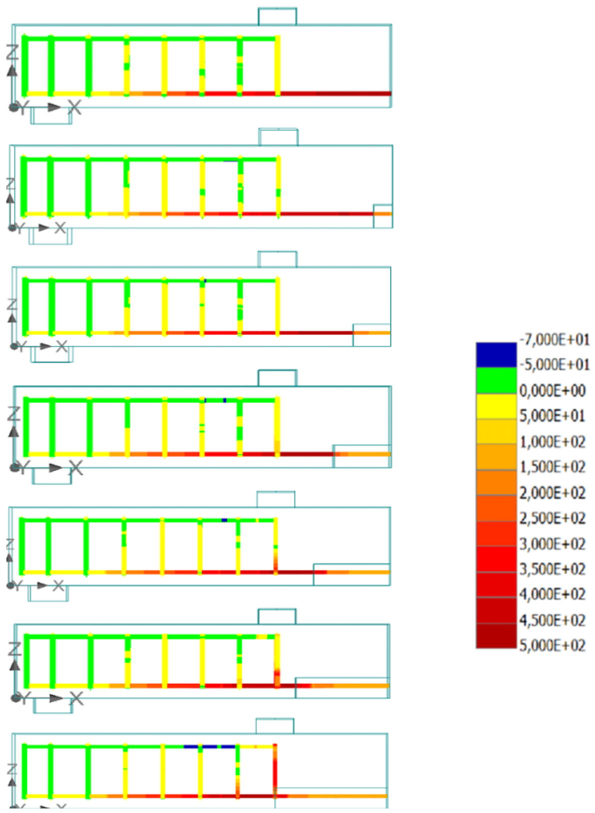

Fig. 10. Reinforcement stress of beam with various patching lengths.

Figure 11 shows the maximum load that reinforced concrete beams can withstand for various patching lengths. The load value (P) in the figure has been normalized to the maximum capacity of the beam without repair (P_o). As can be seen from the figure, the application of a 100 mm patching length seems not to affect the ultimate capacity of the beam. The increase in the flexural capacity of the beam follows the polynomial trend and becomes more pronounced for the patching length of more than 200 mm. The most significant increase occurs when the patching length exceeds the maximum beam moment region. For a patching length of 700 mm, the maximum load may increase by 28% from the ultimate beam capacity without repair.

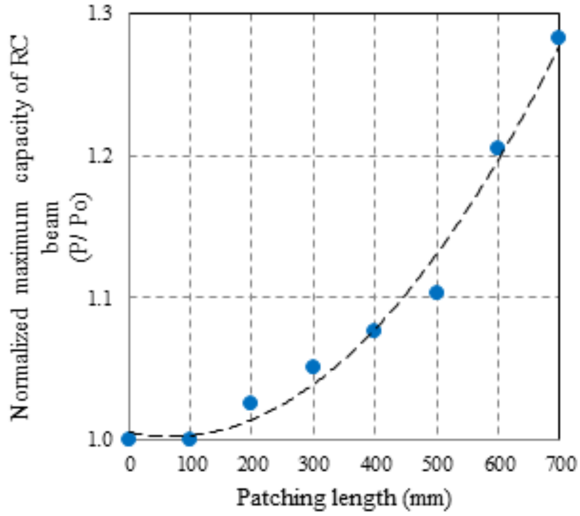

Fig. 11. Influence of patching length.

4. Conclusions

The patched RC beam behaves differently from the normal beam. By utilizing patch repair on the beam, the location of maximum stress can be shifted to the outer limit of the repair zone (which has a smaller bending moment). As a result, the border zone will first undergo cracking and reinforcement yielding. On the other hand, the flexural cracks in the repair zone can be effectively prevented until the beam's failure. The remediation of an RC beam with UPR-mortar patching not only restores but also increases flexural strength. The crack intensity of the patched beam is likewise lower than that of the normal beam. Moreover, the longer the patching length, the longer concrete cracking and reinforcement yielding can be postponed. This can improve the beam's ductility and flexural capacity.

Acknowledgment
The authors express their appreciation to all students and laboratory technical assistants who have already help the experimental work. This research is supported financially by Sebelas Maret University through Riset Fundamental (RFUNS) Grant Numbers 516/UN27.21/PP/2019.

References

1. Al-Gadhib, A., Baluch, M., Rahman, M. "Repair and retrofitting of deteriorated reinforced concrete structures–three case studies". *In: The 6th Saudi Engineering Conference*, KFUPM, Dhahran, 2002.
2. Jumaat, M. Z., Kabir, M., Obaydullah, M., "A review of the repair of reinforced concrete beams". *Journal of Applied Science Research*, 2(6), 2006, pp. 317-326.
3. Haddad, R., Shannag, M., Al-Hambouth, M., "Repair of reinforced concrete beams damaged by alkali-silica reaction". *ACI Structural Journal,* 105(2), 2008, pp. 145.
4. Jassa, P., Beushausen, H., Ngassam, I. T. "Alternative patch repair materials for rebar corrosion damage". *In: MATEC Web of Conferences: EDP Sciences*, 2018, pp. 07017.
5. Kovacs, T., "Deterioration of reinforced concrete repair mortar layers". *Periodica Polytechnica Civil Engineering*, 44(2), 2000, pp. 197-206.
6. O'Dea, V., "Thin-Patch Repair of Concrete in Wastewater Environments Using Commercially Available Cementitious Resurfacers", in *Concrete Repair Bulletin*. 2007, ICRI.
7. Del Vecchio, C., Di Ludovico, M., Pampanin, S., Prota, A., "Repair costs of existing RC buildings damaged by the L'Aquila earthquake and comparison with FEMA P-58 predictions". *Earthquake Spectra*, 34(1), 2018, pp. 237-263.

8. Dolce, M., Goretti, A., "Building damage assessment after the 2009 Abruzzi earthquake". *Bulletin of Earthquake Engineering*, 13(8), 2015, pp. 2241-2264.
9. Bin Jumaat, M. Z., Kabir, M., Obaydullah, M., "Structural performance of reinforced concrete beams repairing from spalling". *European Journal of Scientific Research*, 45(1), 2010, pp. 89-102.
10. Chernin, L., Val, D. V., "Prediction of corrosion-induced cover cracking in reinforced concrete structures". *Construction and Building Materials*, 25(4), 2011, pp. 1854-1869.
11. Chen, Y., Yu, J., Leung, C. K., "Use of high strength strain-hardening cementitious composites for flexural repair of concrete structures with significant steel corrosion". *Construction and Building Materials,* 167, 2018, pp. 325-337.
12. Safehian, M., Ramezanianpour, A. A., "Assessment of service life models for determination of chloride penetration into silica fume concrete in the severe marine environmental condition". *Construction and Building Materials*, 48, 2013, pp. 287-294.
13. Hodhod, O., Ahmed, H., "Modeling the service life of slag concrete exposed to chlorides". *Ain Shams Engineering Journal*, 5(1), 2014, pp. 49-54.
14. Navarro, I. J., Martí, J. V., Yepes, V., "Reliability-based maintenance optimization of corrosion preventive designs under a life cycle perspective". *Environmental Impact Assessment Review*, 74, 2019, pp. 23-34.
15. Bastidas-Arteaga, E., Stewart, M. G., "Damage risks and economic assessment of climate adaptation strategies for design of new concrete structures subject to chloride-induced corrosion". *Structural Safety*, 52, 2015, pp. 40-53.
16. Pelà, L., Aprile, A., Benedetti, A., "Experimental study of retrofit solutions for damaged concrete bridge slabs". *Composites Part B: Engineering*, 43(5), 2012, pp. 2471-2479.
17. Zhu, Y., Zhang, Y., Hussein, H. H., Chen, G., "Flexural strengthening of reinforced concrete beams or slabs using ultra-high performance concrete (UHPC): A state of the art review". *Engineering Structures*, 205, 2020, pp. 110035.
18. Río, O., Andrade, C., Izquierdo, D., Alonso, C., "Behavior of patch-repaired concrete structural elements under increasing static loads to flexural failure". *Journal of materials in civil engineering*, 17(2), 2005, pp. 168-177.
19. Kristiawan, S. A., Saifullah, H. A., Supriyadi, A., "Influence of Patching on the Shear Failure of Reinforced Concrete Beam without Stirrup". *Infrastructures*, 6(7), 2021, pp. 97.
20. Abrian, A. P., Kristiawan, S. A., Saifullah, H. A., Rafi, P. M., Hafizh, R. M., Simanjuntak, A. M., Bismo, D. A. "Experimental Investigation on the Shear Behavior of Patched RC Beams Without Web Reinforcements: Efficacy of Patching Position with Respect to the Shear Span". *In: Proceedings of the 5th International Conference on Rehabilitation and Maintenance in Civil Engineering*, Singapore: Springer Nature Singapore, 2023, pp. 233-242.
21. Amin, M., Zeyad, A. M., Tayeh, B. A., Saad Agwa, I., "Effects of nano cotton stalk and palm leaf ashes on ultrahigh-performance concrete properties incorporating recycled concrete aggregates". *Construction and Building Materials*, 302, 2021, pp. 124196.
22. Amin, M., Zeyad, A. M., Tayeh, B. A., Saad Agwa, I., "Effect of ferrosilicon and silica fume on mechanical, durability, and microstructure characteristics of ultra high-performance concrete". *Construction and Building Materials*, 320, 2022, pp. 126233.
23. Raupach, M., Büttner, T., "Concrete Repair to EN 1504". Boca Taon, Florida 33487-2742: *CRC Press Taylor & Francis Group*, 2014.
24. Kiani, B., Liang, R. Y., Gross, J., "Material selection for repair of structural concrete using VIKOR method". *Case studies in construction materials*, 8, 2018, pp. 489-497.
25. Nabhan, F., "Selection of repair materials using expert advice". *Indian Concrete Journal*, 81(6), 2007, pp. 51-54.
26. Committee, A. C. I., "546R-14: Guide to Concrete Repair". *Technical Documents*, 2014.
27. Institution, B. S., "BS EN 1504-9: 2008 Products and Systems for the Protection and Repair of Concrete Structures–Definitions–Requirements–Quality Control and Evaluation of Conformity–Part 9: General Principles for Use of Products and Systems", *British Standard Institution*, London, UK, 2004.
28. Morgan, D., "Compatibility of concrete repair materials and systems". *Construction and building materials*, 10(1), 1996, pp. 57-67.
29. Venkiteela, G., Klein, M., Najm, H., Balaguru, P. N., "Evaluation of the compatibility of repair materials for concrete structures". *International Journal OF Concrete Structures and materials*, 11(3), 2017, pp. 435-445.
30. Vaysburd, A. M., Bissonnette, B., von Fay, K. F., "Compatibility issues in design and implementation of concrete repairs and overlays": *US Department of the Interior, Bureau of Reclamation, Technical Service,* 2014.
31. Vaysburd, A. M. "Durability of Repaired Concrete Structures–The Battle for Survival". *In: 2nd International RILEM Symposium on Advances in Concrete through Science and Engineering: RILEM Publications SARL*, 2006, pp. 207-224.
32. Vaysburd, A., Emmons, P., Bissonnette, B., Pigeon, M. "Some aspects of evaluating cracking sensitivity of repair materials". *In: International RILEM Conference on Early Age Cracking in Cementitious Systems: RILEM Publications* SARL, 2003, pp. 169-185.
33. Zanotti, C., Rostagno, G., Tingley, B., "Further evidence of interfacial adhesive bond strength enhancement through fiber reinforcement in repairs". *Construction and Building Materials*, 160, 2018, pp. 775-785.
34. Logeswaran, V., Ramakrishna, G., "A Study on Compatibility of Concrete Repair Materials", *Journal of Xi'an University of Architecture & Technology*, 12(6), 2020, pp. 1123-1143.
35. Nunes, V. A., Borges, P. H., Zanotti, C., "Mechanical compatibility and adhesion between alkali-activated repair mortars and Portland cement concrete substrate". *Construction and Building Materials,* 215, 2019, pp. 569-581.
36. Ali, M. S., Leyne, E., Saifuzzaman, M., Mirza, M. S., "An experimental study of electrochemical incompatibility between repaired patch concrete and existing old concrete". *Construction and Building Materials*, 174, 2018, pp. 159-172.
37. Courard, L., Garbacz, A. "Failure of concrete repair: how to avoid it?". In: RILEM PRO 51*: Proc. 2nd Int. Symp. on Advances in Concrete through Science and Eng*, 2006, pp. 167-191.
38. Kristiawan, S. A., Prakoso, A. B. "Flexural behaviour of patch-repair material made from unsaturated polyester resin (UPR)-mortar". *In: Materials Science Forum, Taiwan: Trans Tech Publ*, 2016, pp. 426-430.
39. Kristiawan, S. A., Prakoso, A. B., "Bond strength characteristic of concrete patch repair material made from unsaturated polyester resin (UPR)-mortar". *Applied Mechanics and Materials*, 754, 2015, pp. 442.
40. Saifullah, H. A., Nakarai, K., Piseth, V., Chijiwa, N., Maekawa, K., "Shear Creep Failures of Reinforced Concrete Slender Beams without Shear Reinforcement". *ACI Structural Journal*, 114(6), 2017, pp. 1581-1590.
41. Kristiawan, S., Supriyadi, A., Sangadji, S., Santosa, D. "Cracking behaviour and its effect on the deflection of patched-reinforced concrete beam under flexural loading". *In: MATEC web of conferences: EDP Sciences*, 2017, pp. 02021.
42. Kristiawan, S., Supriyadi, A., Muktamirin, M., "Effect of patching thickness on the flexural performance of patched reinforced concrete beams". Advances in Civil, *Architectural, Structural and Constructional Engineering,* London, UK, 2016, pp. 225-229.
43. Kristiawan, S., Supriyadi, A., Pradana, D. R., Azhim, M. R. N., "Flexural behaviour of one-way patched reinforced concrete (RC) slab under concentrated load". *Asian Journal of Civil Engineering*, 19, 2018, pp. 157-164.
44. Kristiawan, S. A., Supriyadi, A., "Two-way patched RC slabs under concentrated loads". *Magazine of Civil Engineering*, 94(2), 2020, pp. 12.
45. Supriyadi, A., Adi Kristiawan, S., Raditya, S., "Experimental Investigation on the Flexural Behaviour of Patched Reinforced Concrete with Unsaturated Polyester Resin Mortar". *Applied Mechanics and Materials*, 754-755, 2015, pp. 457-462.
46. Sahamitmongkol, R., Suwathanangkul, S., Phoothong, P., Kato, Y., "Flexural Behavior of Corroded RC Members with Patch Repair - Experiments & Simulation". *Journal of Advanced Concrete Technology*, 6(2), 2008, pp. 317-336.
47. Alshaikh, I. M. H., Bakar, B. H. A., Alwesabi, E. A. H., Zeyad, A. M., Magbool, H. M., "Finite element analysis and experimental validation of progressive collapse of reinforced rubberized concrete frame". *Structures*, 33, 2021, pp. 2361-2373.